RESEARCH ARTICLE

Spatial segregation and cooperation in radially expanding microbial colonies under antibiotic stress

Anupama Sharma[a], Kevin B. Wood[a,b,*]
Department of Biophysics, University of Michigan, Ann Arbor, USA[a];
Department of Physics, University of Michigan, Ann Arbor, USA[b]

Email to: K. Wood, kbwood@umich.edu.

ABSTRACT Antibiotic resistance in microbial communities reflects a combination of processes operating at different scales. The molecular mechanisms underlying antibiotic resistance are increasingly understood, but less is known about how these molecular events give rise to spatiotemporal behavior on longer length scales. In this work, we investigate the population dynamics of bacterial colonies comprised of drug-resistant and drug-sensitive cells undergoing range expansion under antibiotic stress. Using the opportunistic pathogen *E. faecalis* with plasmid-encoded (β-lactamase) resistance as a model system, we track colony expansion dynamics and visualize spatial pattern formation in fluorescently labeled populations exposed to ampicillin, a commonly-used β-lactam antibiotic. We find that the radial expansion rate of mixed communities is approximately constant over a wide range of drug concentrations and initial population compositions. Microscopic imaging of the final populations shows that resistance to ampicillin is cooperative, with sensitive cells surviving in the presence of resistant cells even at drug concentrations lethal to sensitive-only communities. Furthermore, despite the relative invariance of expansion rate across conditions, the populations exhibit a diverse range of spatial segregation patterns, with both the spatial structure and the population composition depending on drug concentration, initial composition, and initial population size. Simple mathematical models indicate that the observed dynamics are consistent with global cooperation, and experiments confirm that resistant colonies provide a protective effect to sensitive cells on length scales multiple times the size of a single colony. Furthermore, in the limit of small inoculum sizes, we experimentally show that populations seeded with (on average) no more than a single resistant cell can produce mixed communities in the presence of drug. Our results suggest that β-lactam resistance can be cooperative even in spatially extended systems where genetic segregation typically disfavors exploitation of locally produced public goods.

INTRODUCTION

Antibiotic resistance is increasingly viewed as a long-term threat to global health (1, 2). Thanks to decades of seminal breakthroughs in microbial genetics and molecular biology, the molecular-scale conduits of resistance are often well-understood (3), though the diversity and ubiquity of these defense systems paints a dauntingly complex picture of microbial adaptability. In addition, antibiotic resistance can reflect collective phenomena (4, 5, 6, 7, 8, 9, 10, 11, 12), leading to microbial communities that are significantly more resilient than the individual constituent cells. As a result, there is a growing need to understand dynamics of resistance–and of microbial populations in

general–across length scales.

In nature bacterial populations frequently exist as spatially structured populations called biofilms. Biofilms exhibit a fascinating array of spatiotemporal behavior borne from a combination of heterogeneity, competition, and collective dynamics across length scales (13, 14, 15, 16, 17, 18, 19, 20, 21, 22, 23, 24). Biofilms also contribute to a wide range of clinical complications, including infections of heart valves and surgical implants (25, 26). Work over the last 20 years, in particular, has dramatically improved our understanding of spatial segregation, selection, cooperation, and genetic drift in expanding microbial communities (27, 28, 29, 30, 31, 32, 33, 34, 35, 36, 37, 38, 24). These dynamics often reflect locally heterogeneous cell-cell interactions which lead to emergent behavior on longer length scales. During range expansions of bacterial colonies, the enhanced genetic drift at the growing front frequently gives rise to large spatial sectors of cells from a common lineage (28), though range expansions can either maintain or decrease population diversity depending on the nature and scale of intercellular interactions (28, 34, 33, 39, 37).

Despite an increasingly mature understanding of spatial dynamics in microbial communities, much of our knowledge of antibiotic resistance is derived from experiments in homogeneous (well-mixed) liquid cultures. However, numerous studies indicate that spatial heterogeneity in drug concentration can modulate the evolution of resistance (40, 41, 42, 43, 44, 45, 46). More generally, spatial structure can play an important role in the presence of cooperative resistance mechanisms. When resistance is conferred by drug-targeting enzymes that reduce local antibiotic concentration, for example, the dynamics in even well-mixed communities can be complex and counterintuitive (6, 9, 47). Spatial structure can enhance or inhibit these effective intracellular interactions, creating an environment where cooperation, competition, and evolutionary selection are potentially shaped by spatial constraints (48, 49, 50, 51, 52). Unfortunately, the length scales that determine cooperative resistance phenotypes are not well understood, in general, leading to a gap in our understanding of how interactions driven by resistance mechanisms shape the dynamics and evolution of bacterial populations.

In this work, we take a step towards closing this knowledge gap by probing the population dynamics of mixed bacterial colonies comprised of drug-resistant and drug-sensitive cells undergoing range expansion under antibiotic stress. As a model system, we use *E. faecalis*, a Gram-positive opportunistic pathogen (53) that readily forms biofilms associated with clinical infections (54, 55, 56). Specifically, we track colony expansion dynamics and visualize spatial pattern formation in fluorescently labeled populations exposed to ampicillin, a commonly-used β-lactam antibiotic. Populations are comprised of two strains mixed in varying proportions; one strain is sensitive to ampicillin, while the other is engineered to constitutively express plasmid-encoded β-lactamase, an enzyme which confers ampicillin resistance by hydrolyzing the drug's β-lactam ring (57, 58, 59). Surprisingly, we find that the radial expansion rate of mixed communities is approximately constant over a wide range of drug concentrations and (initial) population compositions. Microscopic imaging of the final populations shows that resistance to ampicillin is cooperative, with sensitive cells surviving in the presence of resistant cells even at drug concentrations lethal to sensitive-only communities. Furthermore, despite the relative invariance of expansion rate across conditions, the populations exhibit a diverse range of spatial segregation patterns, with both the spatial structure and the population composition depending on drug concentration, initial composition, and initial population size. Simple mathematical models indicate that the observed dynamics are consistent with global cooperation, and experiments

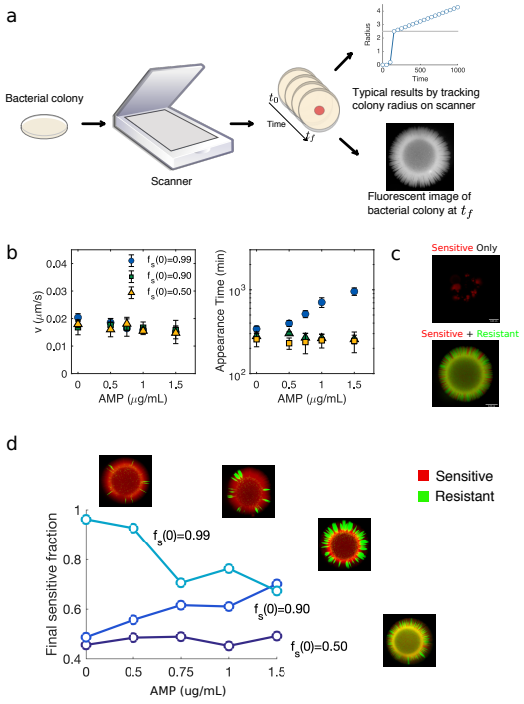

FIG 1 Varying drug concentration and initial resistance fraction alters population composition and appearance time but not expansion velocity. a. Schematic of experimental setup. Colonies are grown on BHI-agar plates and imaged over time using a computer controlled document scanner, allowing for an estimate of the radial expansion velocity and appearance time. At the final time point, the colony is imaged using a fluorescence microscope. b. Expansion velocity (left) and appearance time (right) of mixed colonies containing drug sensitive (WT) and drug resistant (β-lactamase producing) strains at different starting ratios (sensitive fraction $f_s(0) = 0.99$ (circles), 0.90 (squares), or 0.50 (triangles)) at different ampicillin (AMP) concentrations. c. A sample fluorescence microscopy image of a sensitive only ($f_s(0) = 1$) and a mixed population after growth at super-inhibitory concentrations of AMP (1.5 μg/mL). d. Final sensitive fraction as a function of AMP for populations starting with initial sensitive fractions 0.99 (light blue), 0.90 (blue), 0.50 (dark blue). Images, clockwise from upper right: AMP=0, $f_s(0) = 0.99$; AMP=0.5, $f_s(0) = 0.99$; AMP=1.5, $f_s(0) = 0.99$; AMP=1.5, $f_s(0) = 0.50$. All colonies were started from 2 μL of population standardized to a density of OD=0.1 (the inoculum contained approximately 2×10^5 cells).

confirm that resistant subpopulations–at times originating from only a single resistant cell–provide a protective effect to sensitive cells on length scales multiple times the size of a single colony.

RESULTS

To investigate the dynamics of *E. faecalis* populations exposed to β-lactams, we used a previously engineered drug resistant *E. faecalis* strain that contains a multicopy plasmid that constitutively expresses β-lactamase and also expresses a green (GFP-derived) fluorescent marker (Methods). Sensitive cells harbored a similar plasmid that lacks the β-lactamase insert and expresses a variant of RFP. We grew mixed populations containing sensitive and resistant cells on BHI-agar plates supplemented with various concentrations of antibiotic. We tracked colony growth for 6-7 days post-inoculation using a commercial document scanner, which allowed to us estimate radial expansion velocity and colony appearance time (60), and we then imaged the mixed population

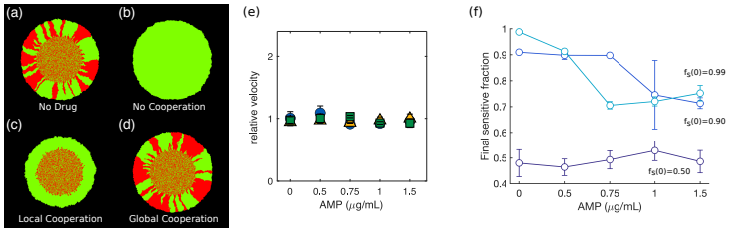

FIG 2 Simulations show long-range cooperative resistance leads to invariant expansion velocity, spatial patterns, and drug-dependent population composition. (a) Simulated colony consisting of drug-sensitive (red) and drug-resistant cells in the absence of drug. (b) In the absence of cooperation, sensitive cells cannot survive at super-inhibitory drug concentrations. (c) Locally cooperative drug resistance, where resistant cells protect neighboring drug sensitive cells from drug-induced cell death, leads to co-existence in the homeland region but drug sensitive cells are not able to survive in the peripheral expanding region. (d) Long-range cooperative resistance, where sensitive cells can survive when the global fraction of resistant cells eclipses a critical threshold, produce spatial patterns similar to those in the absence of drug. Long-range cooperative resistance leads to populations with drug-independent expansion velocity (e) and compositions that depend on drug concentration and initial resistance (f). Expansion velocity is normalized to 1 in the case of no drug.

at the final time point using fluorescence microscopy (Figure 1(a)) and quantified the relative proportion of sensitive and resistant populations (Methods).

Expansion velocity but not population composition is invariant across drug concentrations and initial resistance fractions. Surprisingly, we found that the expansion rate of mixed populations was largely insensitive to initial population composition and drug concentration, including at concentrations that exceed the minimum inhibitory concentration (MIC) for sensitive only populations (Figure 1b). By contrast, the appearance time of the colonies–that is, the time at which the colony is first detected on the scanner–increases at super-MIC concentrations when the initial resistant fraction is sufficiently small (1 percent). Interestingly, the mixed communities contain sensitive cells following growth in ampicillin that would be lethal to sensitive-only populations (Figure 1c), suggesting that resistance is cooperative, with resistant cells offering a protective effect to sensitive cells. However, the composition of the final population can depend significantly on both drug concentration and initial resistant fraction (Figure 1d).

Observed spatial patterns are consistent with long-range cooperative resistance. To make sense of the experimental observations, we developed a simple agent-based model for microbial range expansions in populations of sensitive and resistant cells (Methods). Briefly, the model assumes cell division-driven expansion along with drug concentration-dependent cell death (in sensitive, but not resistant, cells). In the absence of drug, simulations show the expected genetic segregation characteristic of range expansions (Figure 2a). When exposed to super-inhibitory concentrations of antibiotic, resistant cells preferentially survive, leading to homogeneous populations inconsistent with experimental observations (Figure 2b). To incorporate cooperative resistance, we modified the model so that the rate of cell death of sensitive cells is dependent on either 1) the number of resistant cells in the local neighborhood (“local model") or 2) the number of resistant cells in the entire community (“global model"). Simulations of the local model reveal co-existence of sensitive and resistant cells in the homeland region where the initial inoculum was placed, but expansion to larger regions is dominated by resistant cells (Figure 2c), a finding that is again inconsistent with

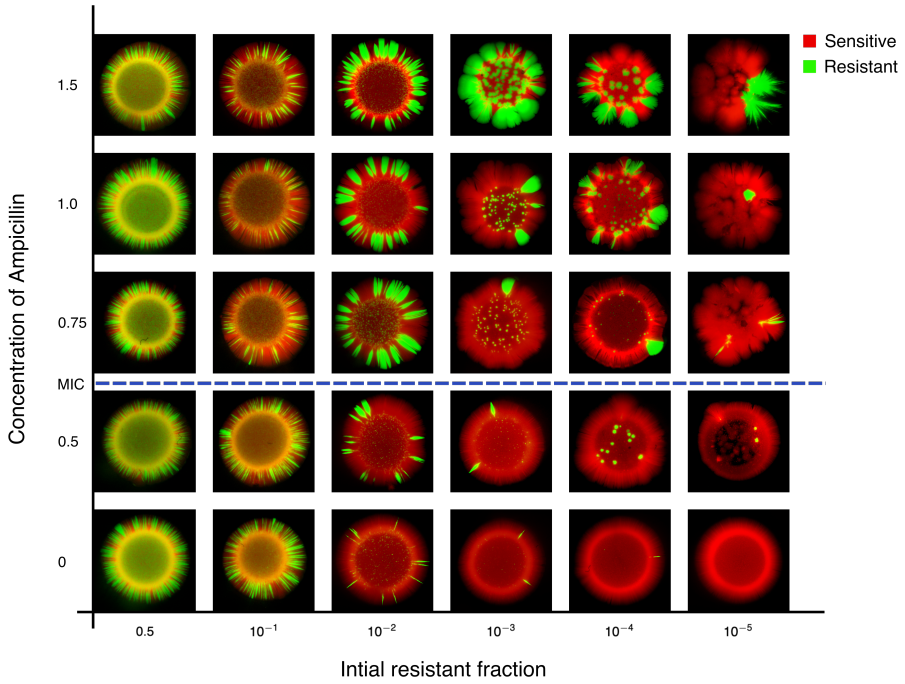

FIG 3 Spatial patterns depend on drug concentration and initial resistant fraction. Images of spatially extended colonies for different concentrations of AMP (vertical axis) and different initial compositions (sensitive fraction increases left to right). Sensitive (red, RFP) and resistant strains (green, GFP) constitutively express different fluorescent proteins. Dashed line indicates the approximate minimum inhibitory concentration (MIC); when drug concentration exceeds the MIC, sensitive-only populations are unable to form colonies (see, for example, Figure 1C). All colonies were started from 2 μL of population standardized to a density of OD=0.1 (the inoculum contained approximately 2×10^5 cells).

observed patterns. By contrast, the global model produces spatial segregation similar to those produced in the absence of drug (Figure 2d). Consistent with experiment, we also find that the globally coupled model leads to expansion velocities invariant across drug concentrations and initial resistant fractions, though the final population composition depends on both factors. Taken together, these simulations suggest that the experimental population dynamics are driven by long-range cooperative resistance between resistant and sensitive cells.

To investigate the nature of the spatial patterns over a wider range of parameters, we grew and imaged colonies starting from initial resistant fractions as small as 10^{-5} for five different concentrations of ampicillin, including both sub- and super-MIC concentrations. In the absence of drug, colonies starting at the lowest resistant fractions contain no visible resistant cells, though all colonies grown above the MIC contain at least one visible resistant subpopulation. We find that the range expansions typically give rise to the smooth wavefronts and sharp domain boundaries that rarely collide and annihilate (Figure 3), as expected for non-motile cells such as *E. faecalis*. Moreover, in the limit of small initial resistant fraction and super-MIC drug concentrations, several populations are characterized by a single localized region of resistant cells within a largely sensitive population. These patterns are consistent with long-range cooperative interactions and suggest that the protective effects of resistant cells extend for nearly the entire length of the colony. In this scenario, survival of the population requires a sufficiently large subpopulation of resistant cells–in the extreme case when initial resistant fraction is 10^{-5}, initial populations contain fewer than 10 resistant cells, on average–though in

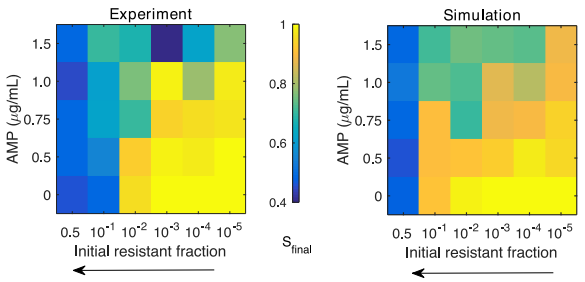

FIG 4 Experiments and simulations show that final composition depends on drug concentration and initial resistant fraction. Heat maps for experiment (left) and simulation (right) indicate final sensitive fraction (S_{final}) for different values of AMP concentration and initial resistant fraction (which increases right to left, as in Figure 3).

the final population these subpopulations need not be spatially distributed (as would be required if cooperation were strictly local). Throughout this regime, final composition is dependent on both initial resistant fraction and drug concentration, and these qualitative trends are also captured by the simulations (Figure 4).

Resistant colonies offer protective effects over length scales several times the size of a single colony. Our results suggest that resistant cells offer cooperative resistance to sensitive cells over relatively long length scales. To directly probe the scale of this interaction, we inoculated one sensitive-only population and one resistant-only population on BHI agar plates supplemented with super-MIC concentrations of ampicillin. The colonies were inoculated at a fixed separation distance, which we varied from 1 to 3 cm, and we then tracked the area of the sensitive colony (in total pixel count) each day (Figure 5). At these drug concentrations, sensitive populations are unable to grow in isolation; any growth therefore reflects protective effects of the nearby resistant colonies. As a control, we also performed identical experiments in the absence of drug. We found that sensitive populations separated by up to 2 cm exhibited substantial growth at the end of the 6 day period, reaching nearly half the size of sensitive colonies grown without drug. By contrast, colonies separated by 3 cm–despite showing growth for the initial 3 days–eventually collapsed. These results indicate that on the timescale of our experiments, resistant colonies exhibit protective effects that extend several centimeters–many times the size of a single microbial colony.

Inoculum density modulates segregation patterns and appearance time with little effect on expansion velocity. In addition to initial resistant fraction, the patterns of segregation are likely to be impacted by the initial density of the total population (i.e. the inoculum density) (61). To investigate this dependence, we grew colonies starting from initial densities that varied over 3 orders of magnitude both with and without super-MIC concentrations of drug. These densities correspond to initial populations containing, on average, between 20 (density of 10^{-4}) and 2×10^5 (density of 0.1) founder cells. Consistent with results in other (non-antibiotic) systems (61), we found that segregation is increased as initial density is decreased, both with and without drug, leading to patterns with thicker sectors (Figure 6). In addition, the expansion velocity was approximately constant across conditions, while arrival time decreased approximately logarithmically with initial density. If we assume that populations are growing at an effective exponential rate k and that arrival time corresponds to the population reaching some critical populations size (i.e. a visible threshold), the slope of the appearance time vs. log(density) plot provides an estimate of $1/k$. For the conditions we measured,

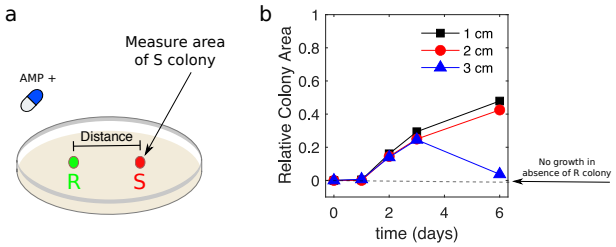

FIG 5 Sensitive colonies grow at super-MIC drug doses when separated from resistant colonies by multiple colony lengths. a. Resistant (green) and sensitive (red) populations are inoculated on day 0 at a fixed separation distance (1, 2, or 3 cm) on BHI-agar plates containing a super-MIC concentration of AMP (1.5 μg/mL). The total area of the sensitive colony (in pixels) is measured daily. For comparison, an identical experiment is also performed in the absence of AMP. b. Area of the sensitive colony over time. Area is normalized by the area of sensitive colonies during a matched control experiment in the absence of drug. Colony area of one indicates growth is identical to that of sensitive colonies in the absence of drug. Note that in the absence of the resistant colony, the sensitive colony is not visible (dashed line).

$k \approx 0.02$ min^{-1}, which corresponds to an approximate doubling time of 35 minutes, only slightly slower than drug-free growth in liquid media at the same temperature.

Initial populations unlikely to contain more than a single resistant cell can survive at super-MIC drug concentrations. We also investigated the combined effects of very small resistant fractions ($< 10^{-2}$) and small inoculum densities, leading to extreme scenarios where the expected number of resistant cells in the initial population is much less than 1. Populations starting from 1 percent resistant cells expand at rates comparable to, but slightly less than, those observed for more resistant populations at the largest initial densities ($> 10^{-2}$), though the arrival time of these colonies is significantly increased in the presence of drug (Figure 7a). For smaller inoculum densities, the colonies cannot be consistently tracked on the scanner, though microscopy images indicate coexistence of both sensitive and resistant cells. If we consider even smaller initial resistant fractions, we eventually reach a limit where growth is completely absent (Figure 7b)–results that are consistent with the fact that populations are unlikely to contain even a single resistant cells at inoculation. In this regime, the populations that do survive contain a single localized subpopulation of resistant cells, indicating that even a single resistant cell in the inoculum can provide sufficient protection to seed colony growth. Because these experiments are performed at super-MIC AMP concentrations, where sensitive cells are unable to survive in the absence of resistant cells, these local islands of resistance again suggest that protection is a long-range phenomenon that does not require sensitive and resistant cells to be in close spatial proximity.

DISCUSSION

Our results complement a number of recent studies showing that antibiotic resistance in microbial communities can reflect cooperative interactions between resistant and sensitive cells (4, 5, 6, 7, 8, 9, 10, 11, 12, 47). The genetic segregation characteristic of many spatially-extended microbial systems often leads to scenarios where “producer cells", those cells that supply a public good such as a drug-degrading enzyme, preferentially benefit other producers, maintaining cooperation and discouraging exploitation by non-producers (30, 15). While we observe the formation of spatial sectors of sensitive or resistant cells, particularly in larger populations, we also observe widespread survival of sensitive cells in mixed populations, even at drug concentrations lethal

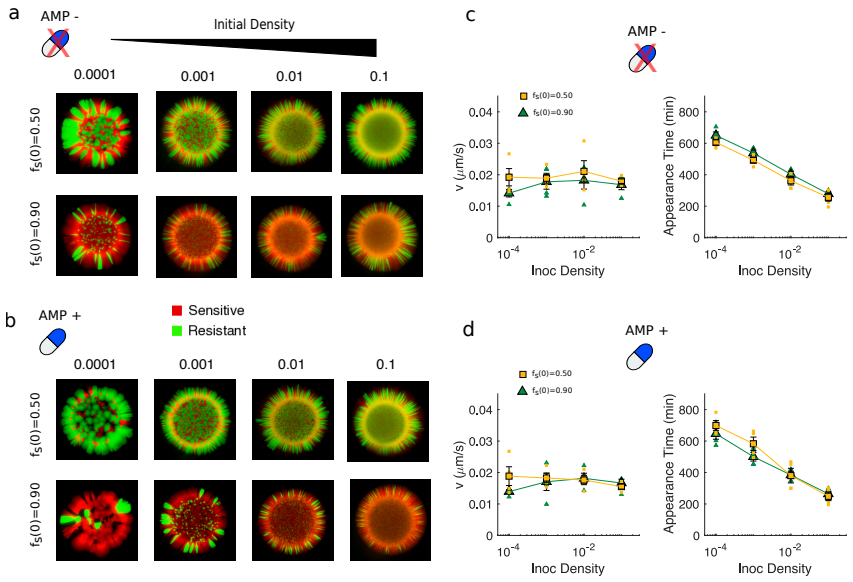

FIG 6 Decreasing inoculum density leads to increased segregation and faster appearance times but little change in expansion velocity. a. Spatial patterns for colonies starting from initial sensitive fractions of 0.5 (top) or 0.9 (bottom) and different starting (total) densities (increasing left to right) in the absence of AMP. b. Same as panel a, but in the presence of AMP at super-MIC concentrations (1 μg/mL). c. Radial expansion velocity (left) and appearance time (right) for colonies grown under the same conditions as in panel a. Small points are individual replicates, large markers are mean over replicates ± standard error of the mean. Appearance time depends logarithmically on initial density, and the slope of the line is consistent with a per capita growth rate of approximately 0.02 min^{-1} (doubling time approximately 35 minutes). d. Same as panel c, but in the presence of super-MIC AMP.

to sensitive-only populations. The ubiquity of these non-producers can be partially explained by the presence of long-range cooperative interactions, where resistant cells offer a protective effect that extends far beyond their neighboring cells–extending for up to several centimeters on the timescales of our experiments. It is perhaps surprising to see such long-range effects, particularly because β-lactamase producing *E. faecalis* are generally not motile and are not believed to release the enzyme into the extracellular space (57, 59). Cooperation is therefore unlikely to result from long-range diffusion of the enzyme itself, but instead from diffusion of drug molecules to spatially fixed "sinks" (resistant cells) where they are degraded. In systems where the cells are motile or the enzyme can freely diffuse, the dynamics of cooperation may be considerably more complex and even, in some limits, mimic behavior of classic reaction-diffusion (or even sub-diffusive) systems (62, 63).

It is important to keep in mind several limitations of our study. Perhaps most importantly, this work is entirely *in vitro* and therefore does not capture the complex environmental factors that may drive the formation of biofilms–and the expansion of resistance–in clinical scenarios. In particular, the range and magnitude of cooperative interactions may depend on specific conditions–dictated, for example, by diffusion constants and growth rates characteristic of a given host environment–potentially leading to different dynamics. In addition, our experiments take place on relatively short timescales, where population behavior is likely dominated by selection of existing resistant strains rather than evolution of new resistance mutations. Our results may not, therefore, reflect dynamics that are stable on evolutionary timescales, where stochastic appearance of new phenotypes may lead to entirely new behavior. Finally,

we note that the simple mathematical model used here neglects many known features of the antibiotic response in living microbial communities, including pharmacological details of drug activity and phenotypic heterogeneity. Nevertheless, the minimal model reproduces many of the observed qualitative trends and, along with experiments, supports the idea that interactions between resistant and sensitive *E. faecalis* communities promote survival of drug sensitive cells on length scales the size of entire communities.

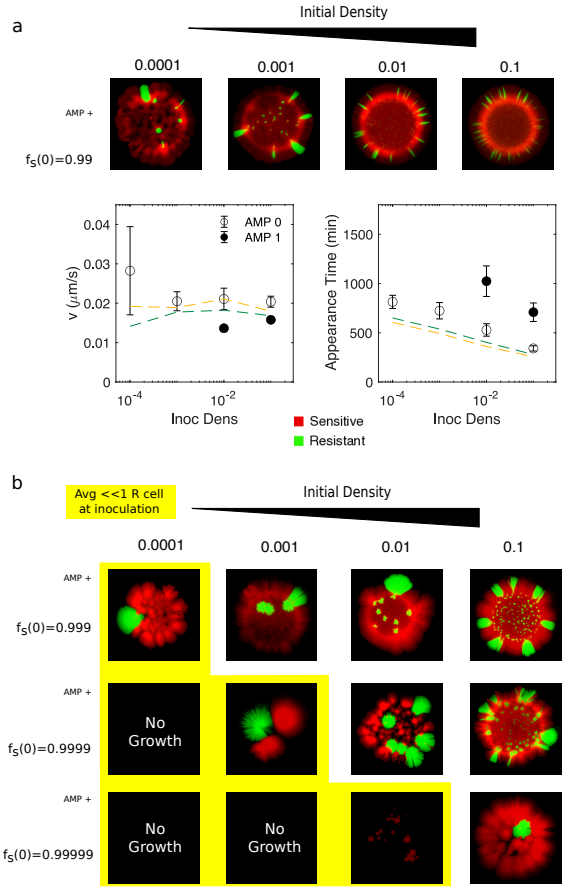

FIG 7 Initial populations unlikely to contain more than a single resistant cell are able to survive super-MIC concentrations a. Colonies formed in the presence of super-MIC AMP (1 μg/mL) starting from populations with one percent resistant cells at different total densities (left to right, corresponding to initial population sizes ranging from 10s to hundreds of thousands of cells). Bottom panels, expansion velocity (left) and appearance time (right) for colonies grown with (closed circles) and without (open circles) super-MIC AMP. Dashed lines (yellow, $f_s(0) = 0.5$; green, $f_s(0) = 0.9$) indicate mean trends from Figure 6 for comparison. Note that for initial densities less than 0.01, low colony density prohibits estimates of arrival time and expansion velocity on the scanner. b. Similar to panel a, but for increasingly smaller initial resistant fractions. Yellow region highlights conditions where initial population is unlikely to contain more than a single resistant cell (expected number $\langle R_0 \rangle \ll 1$). See also Figures S1- S2 for complete data set and drug-free controls.

METHODS

Bacterial strains and growth conditions Experiments were performed with *E. faecalis* strain OG1RF. Ampicillin resistant strains were engineered as described in (47). Briefly, we transformed (64) OG1RF with a modified version of the multicopy plasmid pBSU101, which was originally developed as a fluorescent reporter for Gram-positive bacteria (65). The modified plasmid, named pBSU101-BFP-BL, expresses BFP (rather than GFP in the original plasmid) and also constitutively expresses β-lactamase driven by a native promoter isolated from the chromosome of clinical strain CH19 (58). The β-lactamase gene and reporter are similar to those found in other isolates of enterococci and streptococci (57, 66). Similarly, sensitive strains were transformed with a similar plasmid, pBSU101-DasherGFP, a pBSU101 derivative that lacks the β-lactamase insert and where eGFP is replaced by a brighter synthetic GFP (Dasher-GFP; ATUM ProteinPaintbox, https://www.atum.bio/). The reporter plasmids are described in detail in (67). The plasmids also express a streptomycin resistance gene, and all media was therefore supplemented with streptomycin.

Antibiotics Antibiotics used in this study included Spectinomycin Sulfate (MP Biomedicals) and Ampicillin Sodium Salt (Fisher).

Colony growth experiment Colony-growth experiments were conducted on 1% agar plates with Brain-Heart Infusion media (Remel) at 36C. Plates were poured 1 day before inoculation and stored at -30C. Cells of both strains were grown at 36C overnight in liquid BHI and spectinomycin. On the day of inoculation on agar plates, the overnight culture was diluted in fresh media and spectinomycin, and was grown for 3 hrs to ensure that the cells are in the exponential phase. 1 mL of this diluted culture was spun down for 3 min at $6800 \times g$ and re-suspended in 1 mL of NFW. The densities of such suspensions were measured and adjusted to OD_{600} of 0.1 by adding or removing NFW as needed. Thereafter, the suspensions were mixed in the desired ratios and a droplet of volume $2\ \mu L$ was pipetted onto the agar plate.

Image acquisition and analysis A commercial document scanner controlled by a computer program was used to take time series of images for several days (60). These images were then processed and used to estimate the colony growth rate and appearance time using custom analysis scripts based in Fiji and Matlab. At the end of the expansion experiment (marked by no change in colony radius), the colonies were visualized under a fluorescence stereoscope (Olympus SZX16). The acquired images were processed in Fiji and Matlab.

Cooperative growth model To simulate the colony growth dynamics of a mixed microbial population, we developed a simple agent based model of microbial range expansions, similar to the Eden growth model (68). Our goal is not to produce the fine-scale quantitative features of the observed spatial patterns, which may require more detailed models. Instead, our aim was to develop a minimal model to probe the qualitative features of our experiments, most notably the observations that 1) population composition, but not expansion velocity, depends on drug concentrations and initial resistant fraction and 2) spatial patterns are consistent with long-range cooperative resistance.

We begin with an initial population consisting N_0 individual cells arranged within a circle of radius r on a two-dimensional lattice. This initial population consists of two subpopulations representing drug-sensitive cells (labeled by -1) and drug-resistant cells (labeled by $+1$). Each lattice site is occupied by only one type of allele and unoccupied sites are represented by 0. At each time step, a random cell is selected for division, which populates one of the unoccupied neighbouring sites (8 nearest neighbors, in total) by a cell of the same type ($\varnothing \rightarrow \pm 1$). To model growth in super-MIC

drug concentrations, sensitive cells are also allowed to die ($-1 \rightarrow \varnothing$) with probability d, which depends on drug concentration. For simplicity, we assume d is proportional to AMP concentration, with the proportionality constant chosen so that sensitive-only populations cannot survive at AMP concentrations greater than the MIC.

To incorporate cooperative resistance between resistant and sensitive cells, we assume that the death probability d for sensitive cells depends on the local population of resistant cells. In the local version of the model, the death rate depends only on the fraction of nearest neighbor cells that are resistant, while the global version depends on the fraction of resistant cells in the entire population. For simplicity, we assume a simple threshold model where death of sensitive cells occurs at a rate d when the fraction of resistant cells is small but drops to 0 (i.e. the sensitive cell acts like a resistant cell) when the resistant fraction crosses some threshold f_{crit}. Because this threshold may also depend on drug concentration–intuitively, larger drug concentrations would require larger populations of resistant cells to degrade drug to sub-MIC levels–we also take the threshold to be proportional to AMP concentration.

ACKNOWLEDGMENTS

This work is supported by the National Science Foundation (NSF No. 1553028 to KW), the National Institutes of Health (NIH No. 1R35GM124875-01 to KW), and the Hartwell Foundation for Biomedical Research (to KW). We would like to thank Dr. Wen Yu for her initial work in troubleshooting the document scanner system for tracking colony growth, and members of the Wood lab (UM) for helpful discussions. The format for this preprint is adapted from the American Society for Microbiology (ASM) template available on Overleaf.com.

REFERENCES

1. Levy SB, Marshall B. Antibacterial resistance worldwide: causes, challenges and responses. Nat. medicine 2004; 10(12s):S122.
2. Davies J, Davies D. Origins and evolution of antibiotic resistance. Microbiol. Mol. Biol. Rev. 2010; 74(3):417–433.
3. Blair JM, Webber MA, Baylay AJ, Ogbolu DO, Piddock LJ. Molecular mechanisms of antibiotic resistance. Nat. reviews microbiology 2015; 13(1):42.
4. Mah TFC, O'Toole GA. Mechanisms of biofilm resistance to antimicrobial agents. Trends microbiology 2001; 9(1):34–39.
5. Lee HH, Molla MN, Cantor CR, Collins JJ. Bacterial charity work leads to population-wide resistance. Nature 2010 Sep; 467(7311):82–85. http://dx.doi.org/10.1038/nature09354.
6. Yurtsev EA, Chao HX, Datta MS, Artemova T, Gore J. Bacterial cheating drives the population dynamics of cooperative antibiotic resistance plasmids. Mol. Syst. Biol. 2013 Aug; 9. http://dx.doi.org/10.1038/msb.2013.39.
7. Meredith HR, Srimani JK, Lee AJ, Lopatkin AJ, You L. Collective antibiotic tolerance: Mechanisms, dynamics, and intervention. Nat. chemical biology 2015; 11(3):182.
8. Vega NM, Gore J. Collective antibiotic resistance: mechanisms and implications. Curr. Opin. Microbiol. 2014; 21:28 – 34. http://www.sciencedirect.com/science/article/pii/S1369527414001234, antimicrobials.
9. Sorg RA, Lin L, van Doorn GS, Sorg M, Olson J, Nizet V, Veening JW. Collective Resistance in Microbial Communities by Intracellular Antibiotic Deactivation. PLOS Biol. 2016 Dec; 14(12):e2000631. http://dx.doi.org/10.1371/journal.pbio.2000631.
10. Udekwu KI, Parrish N, Ankomah P, Baquero F, Levin BR. Functional relationship between bacterial cell density and the efficacy of antibiotics. J. Antimicrob. Chemother. 2009 Feb; 63(4):745–757. http://dx.doi.org/10.1093/jac/dkn554.
11. Tan C, Smith RP, Srimani JK, Riccione KA, Prasada S, Kuehn M, You L. The inoculum effect and band-pass bacterial response to periodic antibiotic treatment. Mol. Syst. Biol. 2012; 8(1).
12. Karslake J, Maltas J, Brumm P, Wood KB. Population Density Modulates Drug Inhibition and Gives Rise to Potential Bistability of Treatment Outcomes for Bacterial Infections. PLoS Comput. Biol 2016; 12(10):e1005098.
13. Donlan RM. Biofilms: microbial life on surfaces. Emerg Infect Dis 2002; 8(9).
14. Stewart PS, Franklin MJ. Physiological heterogeneity in biofilms. Nat. reviews. Microbiol. 2008; 6(3):199.
15. Nadell CD, Drescher K, Foster KR. Spatial structure, cooperation and competition in biofilms. Nat. Rev. Microbiol. 2016; 14(9):589.
16. Chia N, Woese CR, Goldenfeld N. A collective mechanism for phase variation in biofilms. Proc. Natl. Acad. Sci. 2008; 105(38):14597–14602.
17. Martin M, Hölscher T, Dragoš A, Cooper VS, Kovács ÁT. Laboratory evolution of microbial interactions in bacterial biofilms. J. bacteriology 2016; 198(19):2564–2571.
18. Oliveira NM, Martinez-Garcia E, Xavier J, Durham WM, Kolter R, Kim W, Foster KR. Biofilm formation as a response to ecological competition. PLoS Biol 2015; 13(7):e1002191.
19. Thomas VC, Hiromasa Y, Harms N, Thurlow L, Tomich J, Hancock LE. A fratricidal mechanism is responsible for eDNA release and contributes to biofilm development of Enterococcus faecalis. Mol. microbiology 2009; 72(4):1022–1036.
20. Asally M, Kittisopikul M, Rué P, Du Y, Hu Z, Çağatay T, Robinson AB, Lu H, Garcia-Ojalvo J, Süel GM. Localized cell death focuses mechanical forces during 3D patterning in a biofilm. Proc. Natl. Acad. Sci. 2012; 109(46):18891–18896.

21. Prindle A, Liu J, Asally M, Ly S, Garcia-Ojalvo J, Süel GM. Ion channels enable electrical communication within bacterial communities. Nature 2015; 527(7576):59.
22. Liu J, Prindle A, Humphries J, Gabalda-Sagarra M, Asally M, Lee DyD, Ly S, Garcia-Ojalvo J, Süel GM. Metabolic codependence gives rise to collective oscillations within biofilms. Nature 2015; 523(7562):550.
23. Liu J, Martinez-Corral R, Prindle A, Dong-yeon DL, Larkin J, Gabalda-Sagarra M, Garcia-Ojalvo J, Süel GM. Coupling between distant biofilms and emergence of nutrient time-sharing. Science 2017; 356(6338):638–642.
24. Thomen P, Valentin JD, Bitbol AF, Henry N. Spatiotemporal pattern formation in E. coli biofilms explained by a simple physical energy balance. Soft Matter 2020; 16(2):494–504.
25. Donlan RM. Biofilms and device-associated infections. Emerg. infectious diseases 2001; 7(2):277.
26. Costerton JW, Stewart PS, Greenberg EP. Bacterial biofilms: a common cause of persistent infections. Science 1999; 284(5418):1318–1322.
27. Hauert C, Doebeli M. Spatial structure often inhibits the evolution of cooperation in the snowdrift game. Nature 2004; 428(6983):643–646.
28. Hallatschek O, Hersen P, Ramanathan S, Nelson DR. Genetic drift at expanding frontiers promotes gene segregation. Proc. Natl. Acad. Sci. 2007; 104(50):19926–19930.
29. Korolev KS, Avlund M, Hallatschek O, Nelson DR. Genetic demixing and evolution in linear stepping stone models. Rev. modern physics 2010; 82(2):1691.
30. Nadell CD XJ Foster KR. Emergence of Spatial Structure in Cell Groups and the Evolution of Cooperation. PLoS Comput. Biol 2010; 6(3):e1000716.
31. Korolev KS. The fate of cooperation during range expansions. PLoS Comput. Biol 2013; 9(3):e1002994.
32. Korolev KS. Evolution arrests invasions of cooperative populations. Phys. review letters 2015; 115(20):208104.
33. Müller MJ, Neugeboren BI, Nelson DR, Murray AW. Genetic drift opposes mutualism during spatial population expansion. Proc. Natl. Acad. Sci. 2014; 111(3):1037–1042.
34. Momeni B, Brileya KA, Fields MW, Shou W. Strong inter-population cooperation leads to partner intermixing in microbial communities. elife 2013; 2:e00230.
35. Gandhi SR, Yurtsev EA, Korolev KS, Gore J. Range expansions transition from pulled to pushed waves as growth becomes more cooperative in an experimental microbial population. Proc. Natl. Acad. Sci. 2016; p. 201521056.
36. Kayser J, Schreck CF, Gralka M, Fusco D, Hallatschek O. Collective motion conceals fitness differences in crowded cellular populations. Nat. Ecol. & Evol. 2019; 3(1):125–134.
37. Gandhi SR, Korolev KS, Gore J. Cooperation mitigates diversity loss in a spatially expanding microbial population. Proc. Natl. Acad. Sci. 2019; 116(47):23582–23587.
38. Birzu G, Hallatschek O, Korolev KS. Fluctuations uncover a distinct class of traveling waves. Proc. Natl. Acad. Sci. 2018; 115(16):E3645–E3654.
39. Celik Ozgen V, Kong W, Blanchard AE, Liu F, Lu T. Spatial interference scale as a determinant of microbial range expansion. Sci. Adv. 2018; 4(11).
40. Kepler TB, Perelson AS. Drug concentration heterogeneity facilitates the evolution of drug resistance. Proc. Natl. Acad. Sci. 1998; 95(20):11514–11519.
41. Zhang Q, Lambert G, Liao D, Kim H, Robin K, Tung Ck, Pourmand N, Austin RH. Acceleration of emergence of bacterial antibiotic resistance in connected microenvironments. Science 2011; 333(6050):1764–1767.
42. Greulich P, Waclaw B, Allen RJ. Mutational pathway determines whether drug gradients accelerate evolution of drug-resistant cells. Phys. Rev. Lett. 2012; 109(8):088101.
43. Fu F, Nowak MA, Bonhoeffer S. Spatial heterogeneity in drug concentrations can facilitate the emergence of resistance to cancer therapy. PLoS Comput. Biol 2015; 11(3):e1004142.
44. Moreno-Gamez S, Hill AL, Rosenbloom DI, Petrov DA, Nowak MA, Pennings PS. Imperfect drug penetration leads to spatial monotherapy and rapid evolution of multidrug resistance. Proc. Natl. Acad. Sci. 2015; 112(22):E2874–E2883.
45. Baym M, Lieberman TD, Kelsic ED, Chait R, Gross R, Yelin I, Kishony R. Spatiotemporal microbial evolution on antibiotic landscapes. Science 2016; 353(6304):1147–1151.
46. De Jong MG, Wood KB. Tuning spatial profiles of selection pressure to modulate the evolution of drug resistance. Phys. review letters 2018; 120(23):238102.
47. Hallinen KM, Karslake J, Wood KB. Delayed antibiotic exposure induces population collapse in enterococcal communities with drug-resistant subpopulations. bioRxiv 2019; p. 766691.
48. Allen B, Gore J, Nowak MA. Spatial dilemmas of diffusible public goods. Elife 2013; 2:e01169.
49. Frost I, Smith WP, Mitri S, San Millan A, Davit Y, Osborne JM, Pitt-Francis JM, MacLean RC, Foster KR. Cooperation, competition and antibiotic resistance in bacterial colonies. The ISME journal 2018; 12(6):1582–1593.
50. Estrela S BS. Community interactions and spatial structure shape selection on antibiotic resistant lineages. PLoS Comput. Biol 2018; 14(6):e1006179.
51. Amanatidou E, Matthews AC, Kuhlicke U, Neu TR, McEvoy JP, Raymond B. Biofilms facilitate cheating and social exploitation of β-lactam resistance in Escherichia coli. npj Biofilms Microbiomes 2019; 5(1):1–10.
52. Santos-Lopez A, Marshall CW, Scribner MR, Snyder DJ, Cooper VS. Evolutionary pathways to antibiotic resistance are dependent upon environmental structure and bacterial lifestyle. Elife 2019; 8:e47612.
53. Clewell DB, Gilmore MS, Ike Y, Shankar N. Enterococci: from commensals to leading causes of drug resistant infection. Massachusetts Eye and Ear Infirmary; 2014.
54. Huycke MM, Sahm DF, Gilmore MS. Multiple-drug resistant enterococci: the nature of the problem and an agenda for the future. Emerg. infectious diseases 1998; 4(2):239.
55. Mohamed JA, Huang DB. Biofilm formation by enterococci. J. medical microbiology 2007; 56(12):1581–1588.
56. Ch'ng JH, Chong KK, Lam LN, Wong JJ, Kline KA. Biofilm-associated infection by enterococci. Nat. Rev. Microbiol. 2018; p. 1.
57. Murray BE, Mederski-Samaroj B. Transferable beta-lactamase. A new mechanism for in vitro penicillin resistance in Streptococcus faecalis. J. Clin. Investig. 1983 Sep; 72(3):1168–1171. http://dx.doi.org/10.1172/JCI111042.
58. Rice L, Eliopoulos G, Wennersten C, Goldmann D, Jacoby G, Moellering R. Chromosomally mediated beta-lactamase production and gentamicin resistance in Enterococcus faecalis. Antimicrob. agents chemotherapy 1991; 35(2):272–276.
59. Murray BE. Beta-lactmase-producing enterococci. Antimicrob. Agents Chemother. 1992 Nov; 36(11):2355–2359.
60. AU Levin-Reisman I, AU Fridman O, AU Balaban NQ. ScanLag: High-throughput Quantification of Colony Growth and Lag Time. JoVE 2014; (89):e51456.
61. van Gestel J, Weissing FJ, Kuipers OP, Kovács ÁT. Density of founder cells affects spatial pattern formation and cooperation in Bacillus subtilis biofilms. The ISME J. 2014; 8(10):2069–2079.
62. Lindenberg K, West BJ, Kopelman R. Steady-state segregation in diffusion-limited reactions. Phys. review letters 1988; 60(18):1777.
63. Yuste S, Acedo L, Lindenberg K. Reaction front in an A+ B■ C reaction-subdiffusion process. Phys. Rev. E 2004; 69(3):036126.

64. Dunny GM, Lee LN, LeBlanc DJ. Improved electroporation and cloning vector system for gram-positive bacteria. Appl. Environ. Microbiol. 1991; 57(4):1194–1201.
65. Aymanns S, Mauerer S, van Zandbergen G, Wolz C, Spellerberg B. High-level fluorescence labeling of gram-positive pathogens. PLoS One 2011; 6(6):e19822.
66. Zscheck KK, Murray BE. Nucleotide sequence of the beta-lactamase gene from Enterococcus faecalis HH22 and its similarity to staphylococcal beta-lactamase genes. Antimicrob. agents chemotherapy 1991; 35(9):1736–1740.
67. Hallinen KM, Guardiola-Flores KA, Wood KB. Fluorescent reporter plasmids for single-cell and bulk-level composition assays in E. faecalis. bioRxiv 2019; p. 797936.
68. Eden M. A two-dimensional growth process. Dyn. fractal surfaces 1961; 4:223–239.

SUPPLEMENTAL MATERIAL

The Supplemental Material contains 2 supplemental figures.

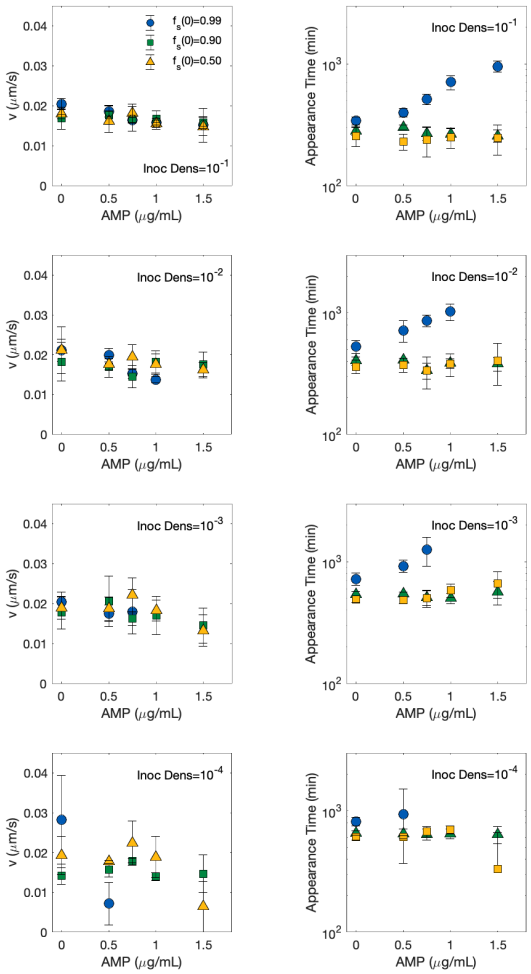

FIG S1 Expansion velocity (left) and appearance time (right) of mixed colonies at different concentrations of ampicillin (AMP). Each row corresponds to a particular inoculum density.

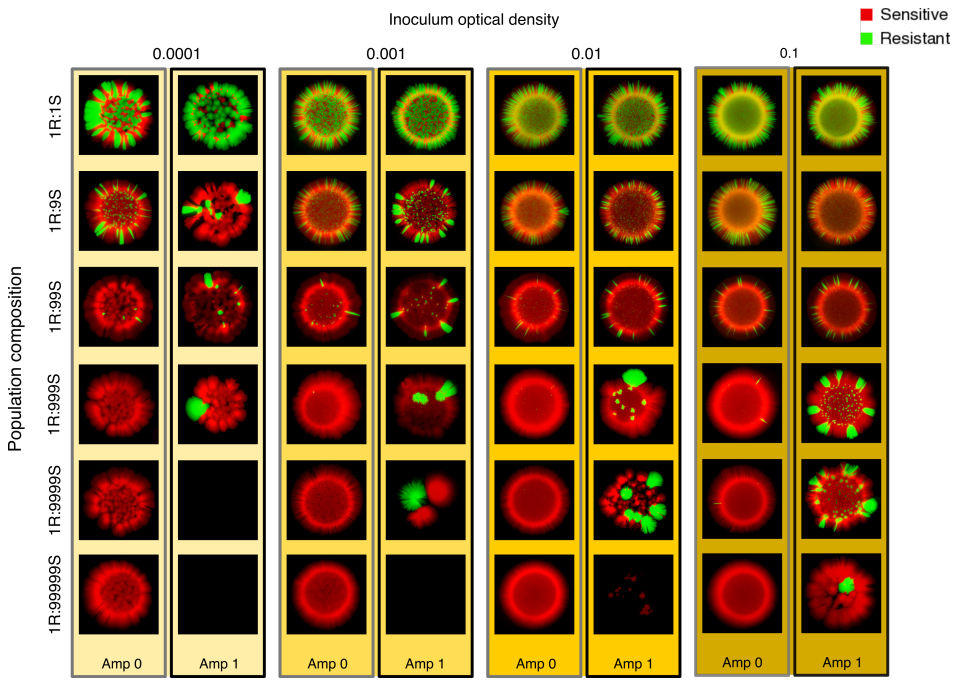

FIG S2 Spatial patterns for example colonies starting from different initial densities (columns) and different initial compositions (rows). For each condition, colonies were grown in the presence or absence of super-MIC AMP (1 *mu*g/mL).